

GA-A27782

**FIRST DIRECT EVIDENCE OF
TURBULENCE-DRIVEN ION FLOW
TRIGGERING THE L- TO H-MODE TRANSITION**

By

L. SCHMITZ, B.A. GRIERSON, L. ZENG, J.A. BOEDO, T.L. RHODES, Z. YAN,
G.R. McKEE, D. ELDON, C. CHRYSTAL, P.H. DIAMOND, W.A. PEEBLES,
G.R. TYNAN, R.J. GROEBNER, K.H. BURRELL, C.C. PETTY, E.J. DOYLE,
and G. WANG

APRIL 2014



DISCLAIMER

This report was prepared as an account of work sponsored by an agency of the United States Government. Neither the United States Government nor any agency thereof, nor any of their employees, makes any warranty, express or implied, or assumes any legal liability or responsibility for the accuracy, completeness, or usefulness of any information, apparatus, product, or process disclosed, or represents that its use would not infringe privately owned rights. Reference herein to any specific commercial product, process, or service by trade name, trademark, manufacturer, or otherwise, does not necessarily constitute or imply its endorsement, recommendation, or favoring by the United States Government or any agency thereof. The views and opinions of authors expressed herein do not necessarily state or reflect those of the United States Government or any agency thereof.

FIRST DIRECT EVIDENCE OF TURBULENCE-DRIVEN ION FLOW TRIGGERING THE L- TO H-MODE TRANSITION

By

L. SCHMITZ,* B.A. GRIERSON,[†] L. ZENG,* J.A. BOEDO,[‡] T.L. RHODES,* Z. YAN,[¶]
G.R. McKEE,[¶] D. ELDON,[‡] C. CRYSTAL,[‡] P.H. DIAMOND,[‡] W.A. PEEBLES,*
G.R. TYNAN,[‡] R.J. GROEBNER, K.H. BURRELL, C.C. PETTY, E.J. DOYLE,*
and G. WANG*

This is a preprint of the synopsis for a paper to be presented at
the Twenty-Fifth IAEA Fusion Energy Conf., October 13-18, 2014
in Saint Petersburg, Russia.

*University of California Los Angeles, Los Angeles, California.
[†]Princeton Plasma Physics Laboratory, Princeton, New Jersey.
[‡]University of California San Diego, La Jolla, California.
[¶]University of Wisconsin-Madison, Madison, Wisconsin.

Work supported by
the U.S. Department of Energy
under DE-FG02-08ER54984, DE-AC02-09CH11466,
DE-FG02-07ER54917, DE-FG02-89ER53296, and DE-FG02-08ER54999

GENERAL ATOMICS PROJECT 30200
APRIL 2014



First Direct Evidence of Turbulence-Driven Ion Flow Triggering the L- to H-Mode Transition

EX-C

L. Schmitz,¹ B.A. Grierson,² L. Zeng,¹ J.A. Boedo,³ T.L. Rhodes,¹ Z. Yan,⁴ G.R. McKee,⁴
D. Eldon,³ C. Chrystal,³ P.H. Diamond,³ W.A. Peebles,¹ G.R. Tynan,³ R.J. Groebner,⁵
K.H. Burrell,⁵ C.C. Petty,⁵ E.J. Doyle,¹ and G. Wang¹

¹University of California Los Angeles, PO Box 957099, Los Angeles, CA 90095-7099, USA
²Princeton Plasma Physics Laboratory, PO Box 451, Princeton, NJ 08543-0451, USA
³University of California San Diego, 9500 Gilman Dr., La Jolla, California 92093-0417, USA
⁴University of Wisconsin-Madison, 1500 Engineering Dr., Madison, WI 53706, USA
⁵General Atomics, PO Box 85608, San Diego, CA 92186-5608, USA
email: lschmitz@ucla.edu

Developing a physics-based model of the L-H transition is critical for confidently extrapolating the auxiliary heating requirements for ITER from the existing empirical L-H transition power threshold scaling. For the first time, it is shown here that the initial (transient) turbulence collapse preceding the L-H transition is caused by turbulence-generated poloidal ion flow and $\mathbf{E} \times \mathbf{B}$ flow *opposing* the equilibrium (L-mode) edge plasma $\mathbf{E} \times \mathbf{B}$ flow. The resulting edge transport reduction *subsequently* results in a periodic increase of the edge pressure gradient ∇P_i , enhancing the diamagnetic (negative) component of the edge electric field and $\mathbf{E} \times \mathbf{B}$ profile shear, and eventually sustaining turbulence suppression and H-mode confinement.

Evidence from several recent experiments has pointed towards a synergistic role of turbulence-driven flows [Zonal Flows (ZFs)] and pressure-gradient-driven flows in the trigger and evolution of the L-H transition. Near power threshold, the transition dynamics is substantially expanded/slowed via limit cycle oscillations (LCO) [1,2], between the turbulence level and the fluid $\mathbf{E} \times \mathbf{B}$ velocity, allowing profile and flow measurements with unprecedented spatial and temporal resolution. Figure 1(a-c) shows the time evolution of the density fluctuation level \tilde{n} and the total $\mathbf{E} \times \mathbf{B}$ velocity as measured by Doppler backscattering (DBS), as well as the $\mathbf{v}_i \times \mathbf{B}$ component of the $\mathbf{E} \times \mathbf{B}$ velocity, calculated from the main ion momentum balance equation $\mathbf{v}_{E \times B} = -1/(Z_i e n_i B) \partial n_i T_i / \partial r + (\mathbf{v}_i \times \mathbf{B})/B$ (where Z_i , n_i , T_i , and \mathbf{v}_i are the main ion charge number, density, temperature and fluid velocity) by subtracting the pressure gradient term from the total $\mathbf{E} \times \mathbf{B}$ velocity. ∇P_i is approximated using the electron density from profile reflectometry (as $Z_{\text{eff}} \sim 1.6$ and $n_{iC} \ll n_i$) and CER carbon ion temperature (assuming $T_{iC} \sim T_i$). Fluctuation suppression is first observed at $t=t_0$ during a positive peak of the $\mathbf{v}_i \times \mathbf{B}$ term. A local $\mathbf{E} \times \mathbf{B}$ flow reversal is also observed at this time [Fig. 1(d)], leading to concomitant large positive and negative shearing rates within a narrow (1 cm) radial region, characteristic of ZF. We show here that the observed positive flow transients are consistent with turbulence-driven poloidal ion flow and $\mathbf{E} \times \mathbf{B}$ flow, and inconsistent with turbulence suppression via diamagnetic (profile) shear in the early LCO phase.

The cross-correlation coefficient of \tilde{n} and the main ion \mathbf{v}_i (via main ion CER) was measured in a helium plasma with dominant ECH.

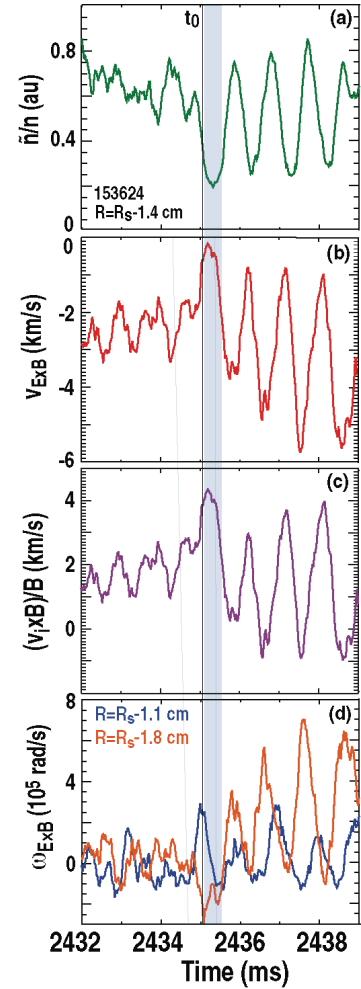


Fig. 1. Time evolution of (a) density fluctuation level; (b) $\mathbf{E} \times \mathbf{B}$ velocity; (c) main ion $\mathbf{v}_i \times \mathbf{B}$ contribution to the $\mathbf{E} \times \mathbf{B}$ velocity; (d) shearing rate $\omega_{E \times B}$ at two radii inside the LCFS. Time of initial turbulence suppression is indicated by a blue bar. R_s is the LCFS radius.

Figure 2(a) shows that v_{i0} lags \tilde{n} after the L-mode-LCO transition and is nearly in phase with $v_{E \times B}$. Both results are consistent with turbulence-driven poloidal flow/ZF according to Eqns (2,4) below. No corresponding correlation of \tilde{n} , $v_{E \times B}$ with the toroidal ion flow is found in the early LCO. Figure 2(b) shows that the total $\mathbf{E} \times \mathbf{B}$ shearing rate leads $-\nabla P_i$ early in the LCO, establishing clearly that the $\mathbf{E} \times \mathbf{B}$ shear modulation early in the LCO is not caused by $-\nabla P_i$ changes. Later in the LCO closer to the final H-mode transition ($t_H = t_0 + 18$ ms), $-\nabla P_i$ increases periodically generating strong negative $\mathbf{E} \times \mathbf{B}$ flow [Fig. 2(c,d), blue bar]. $\omega_{E \times B}$ then lags $-\nabla P_i$. The data suggest that later in the LCO phase, the turbulence growth rate (and \tilde{n}) increase due to the increasing $-\nabla P_i$ within each cycle, in turn driving radial transport and reducing $-\nabla P_i$. The turbulence then collapses due to depletion of turbulence energy [2] as (positive) ZF/poloidal ion flow is driven. Reduced radial transport then allows $-\nabla P_i$ to rise again, transiently maintaining fluctuation suppression via profile shear. Figure 2(e) shows 0-D modeling results of the L-LCO-H-mode transition, using the predator-prey equations (3,4) for the evolution of \tilde{n} and v_{ZF} , along with equations describing diamagnetic flow $v_{\nabla P}$ and poloidal ion flow evolution. In contrast to earlier work [3,4], opposite polarity of ∇P_i -driven and fluctuation-driven $\mathbf{E} \times \mathbf{B}$ /poloidal ion flow is retained here: (1) $\partial \tilde{n} / \partial t = \gamma \tilde{n} - c_1 v_{ZF} \tilde{n} - c_2 v_{\nabla P} - c_3 \tilde{n}^2$, (2) $\partial v_{ZF} / \partial t = c_4 \tilde{n}^2 v_{ZF} - \gamma_D v_{ZF}$; (3) $-\partial v_{\nabla P} / \partial t = Q + c_5 \tilde{n}^2 v_{\nabla P} + c_6 v_{\nabla P}$, and (4) $\partial v_{i0} / \partial t = c_7 \tilde{n}^2 - c_8 v_{i0} - c_9 v_{\nabla P}$. Q is the (slowly increasing) radial heat flux driving the system, and the constants/functions $c_{1..3}$, $c_4 \tilde{n}^2$, γ_D , $c_5 \tilde{n}^2$, c_6 , $c_7 \tilde{n}^2$, c_8 , c_9 describe, in order, shearing via turbulence-driven and diamagnetic flow shear, the nonlinear turbulence saturation rate, the Reynolds stress radial gradient and ZF damping rate, the turbulent and neoclassical radial diffusion rates, poloidal flow drive via the Reynolds stress, and neoclassical poloidal flow damping and gradient drive [4]. Toroidal flow is not included here. Figure 2(e) illustrates that (i) the initial turbulence quench occurs during a positive v_{i0} and $v_{E \times B}$ transient (the latter is observed also in “regular” fast L-H transitions); (ii) the driven ion poloidal flow (blue) opposes $v_{\nabla P}$; (iii) positive v_{i0} (green-blue) and $v_{E \times B}$ (red) excursions lag \tilde{n} (predator-prey relationship) in the LCO as observed experimentally; and (iv) the LCO decreases in frequency (and eventually ceases) due to increasing profile shear ($-\nabla v_{Dia}$, olive), securing the final transition to H-mode. The results reported provide direct evidence of turbulence-driven ZF/main ion flow triggering the LCO, and preceding the transition to H-mode confinement. The results also explain the direction of the \tilde{n} , $v_{E \times B}$ limit cycle observed in the outboard shear layer in DIII-D [1] and recently in JFT-2M [5].

This work was supported by the US Department of Energy under DE-FG02-08ER54984, DE-AC02-09CH11466, DE-FG02-07ER54917, DE-FG02-89ER53296, DE-FG02-08ER54999, and DE-FC02-04ER54698.

- [1] L. Schmitz, et al., Phys. Rev. Lett. **108**, 155002 (2012)
- [2] G. Tynan, et al. Nucl. Fusion **53** 073053 (2012).
- [3] E.J. Kim and P.H. Diamond, Phys. Rev. Lett. **90**, 185006, (2003)
- [4] K. Miki, et al., Phys. Plasmas **19**, 092306 (2012)
- [5] T. Kobayashi, et al., Phys. Rev. Lett. **111**, 035002 (2013).

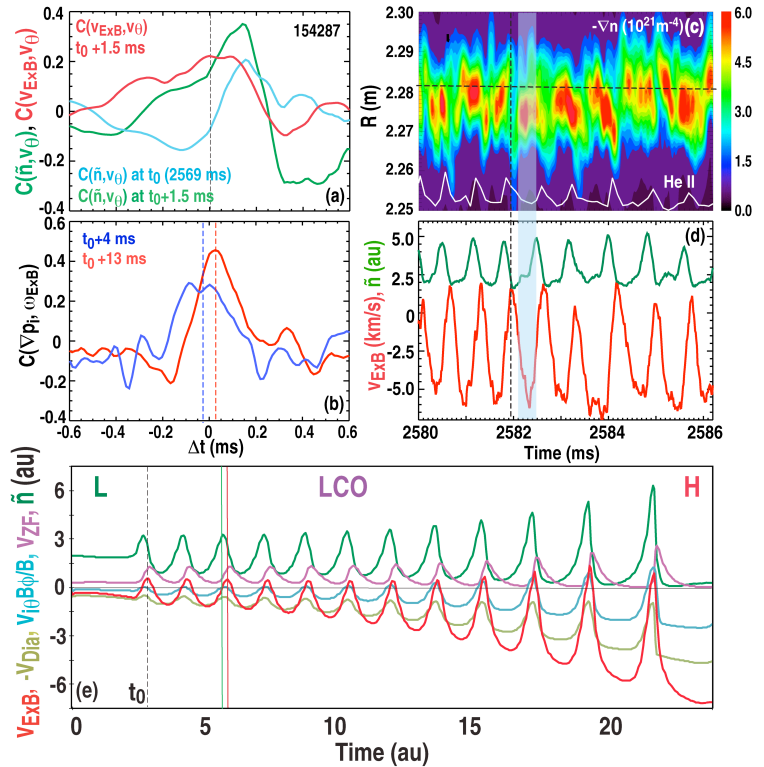


Fig. 2. (a) Correlation coefficient of \tilde{n} and $v_{E \times B}$ with v_{i0} ; (b) correlation of $-\nabla P_i$ with $\omega_{E \times B}$; (c) density gradient and helium II line divertor emission; (d) evolution of \tilde{n} and $v_{E \times B}$; (e) 0-D fluid modeling results as described.